Title: Spatial periodicity in grid cell firing is explained by a neural sequence code of 2D trajectories

Authors: Rebecca R.G.[1], Giorgio A. Ascoli[2], Nate M. Sutton[2], and Holger Dannenberg[2,*]

Affiliations: [1]Department of Mathematical Sciences and [2]Department of Bioengineering, George Mason University, 4400 University Dr., Fairfax, VA 22030
*hdannenb@gmu.edu

Corresponding author: Holger Dannenberg (hdannenb@gmu.edu)

Running head: Axiomatizing grid cells

Keywords: grid cells, cell sequences, path integration, trajectory coding

Conflicts of Interest: The authors declare no competing interests.

ABSTRACT

Spatial periodicity in grid cell firing has been interpreted as a neural metric for space providing animals with a coordinate system in navigating physical and mental spaces. However, the specific computational problem being solved by grid cells has remained elusive. Here, we provide mathematical proof that spatial periodicity in grid cell firing is the only possible solution to a neural sequence code of 2D trajectories and that the hexagonal firing pattern of grid cells is the most parsimonious solution to such a sequence code. We thereby provide a teleological cause for the existence of grid cells and reveal the underlying nature of the global geometrical organization in grid maps as a direct consequence of a simple local sequence code using a minimal number of neurons. A sequence code by grid cells provides intuitive explanations for many previously puzzling experimental observations and may transform our thinking about grid cells.

INTRODUCTION

What is the nature of the problem being solved by grid cells?

Grid cells in the medial entorhinal cortex (MEC)[1,2] and adjacent regions such as the pre- and parasubiculum[3] are hypothesized to supply a "spatial metric" for cognitive map-based navigation and path integration[4–6], episodic memory[7–9], and navigating abstract feature spaces[10–12]. Grid cells recorded in freely foraging animals fire at multiple locations in space so that the firing fields form a hexagonal lattice (**Figures 1A – 1D**). Since their first discovery, the remarkable spatial periodicity in grid cell firing has been a topic of intense research[6]. This research was fueled in part by awe of the beautiful symmetry and complexity displayed in the spatial firing pattern of a single cell. Moreover, research efforts were driven by the hope that understanding the underlying nature of grid cell firing would greatly advance our understanding of how the mammalian brain performs navigational computations and higher cognitive functions such as episodic memory.

However, currently existing mechanistic models of grid cell firing fall short of explaining the basic question of *why* grid cells exist in the first place. Most previous studies on grid cell function follow a traditional approach based on the well-founded assertion in biology that structure determines function. This approach has resulted in a vast literature describing properties of grid cells in multiple species, how these properties depend on internal neural circuit dynamics and external cues, and how grid cell dynamics can be employed for computational or behavioral functions such as memory-guided navigation[4–6] and the planning of direct trajectories to goals[13,14]. However, this traditional approach has been proven notoriously difficult in identifying a teleological cause for the existence of grid cells in mammalian brains, i.e., an explanation of the specific functional purpose they serve. Computational models of grid cells such as oscillatory interference models[15–19] and continuous attractor models[4,20,21] provide mechanistic explanations of how the spatial periodicity in firing can emerge from the structure of microcircuits within the superficial layers of the MEC[22–24]. However, these mechanistic models, too, cannot identify the teleological cause for the emergence of spatial periodicity in grid cell firing. Consequently, functions of grid cells are often explained in generic terms and statements, such as that grid cells supply a path integration-based "metric for space" or provide a "coordinate system" for spatial mapping.

The approach to discover the computational goal of grid cells taken in this study differs from those mechanistic modeling approaches and from traditional approaches in the grid cell literature that aim to assign functions to grid cells based on their properties. Instead, we turn the question on its head and ask the reverse question: What is an important function performed by the mammalian brain that could either not be performed at all or would be substantially more costly or inefficient to perform in the absence of grid cells? This approach follows the logic proposed by David Marr: "To phrase the matter in another way, an algorithm is likely to be understood more readily by understanding the nature of the problem being solved than by examining the mechanism (and hardware) in which it is embodied" (Marr, 2010, Chapter 1.2).

This study provides mathematical proof that, in Marr's words, "the nature of the problem being solved" by grid cells is coding of trajectories in 2D space using cell sequences. By doing so, we offer a specific answer to the question of why grid cells have evolved in the mammalian brain. Thus, we provide a teleological cause for the existence of grid cells.

RESULTS

Spatial periodicity in grid cell firing emerges from a cell sequence code of trajectories in 2D space

To constrain our search for a function that requires grid cells or could not be performed efficiently without grid cells, we reasoned that this function shall rely on sequential activation of grid cells or grid cell assemblies, in short grid cell sequences. This reasoning rests on well-established experimental data on neural activity in the hippocampal formation showing that cell sequences can provide a code for transitional structures of world states, generating an internal representation for memory-guided navigation[26–28]. We further reasoned that, if a fundamental function of grid cells exists, such a function is very likely related to coding of trajectories. This reasoning rests on theoretical work demonstrating that theta sequences of grid cell populations can provide a traveling-direction signal[29], and that temporally structured neural activity in the hippocampal formation may be necessary to temporally bind neural representations of contiguous events[12]. Moreover, data obtained from rodent experiments[30,31] and theoretical work[32] suggest that grid cells serve path integration and memory-guided navigation. A code for spatial trajectories by cell sequences that is usable across different environments would be very useful to keep track of changes in location relative to a starting point, i.e., path integration.

We therefore set out to provide mathematical proof (**Box 1**) that spatial periodicity in grid cell firing emerges from the assertion that cell sequences code for trajectories in 2D space under the constraint that the number of neurons in the brain is finite.

Mathematical proof

Definition 1. Spatial firing field. A spatial firing field of a neuron defines a specific region in space, where a neuron is active, i.e., the neuron responds to a specific spatial location of an animal with an increased rate of action potential firing.

Definition 2.1. Isometry. An *isometry* is a bijective map f that preserves distance, that is for any two points x and y,

$$d(f(x), f(y)) = d(x, y).$$

We say that two geometric figures are *geometrically congruent* if there is an isometry between them. We will abbreviate this to *congruent* in what follows.

The intuitive idea here is that two figures are congruent if one can be laid on top of the other so that they match perfectly. This can be done via rotation, translation, reflection, or a combination of these.

Definition 3.1. Kissing number. Given a geometric figure, the kissing number is the largest number of non-overlapping figures congruent to the original geometric figure that can be arranged in the plane so that they all touch the original geometric figure.

Remark 3.2. This usually refers to spheres embedded in various Euclidean spaces, but here we restrict to the plane and allow convex (see Definition 5) geometric figures other than circles.

Example 3.3. The kissing number of a circle in the plane is 6, which is achieved using a hexagonal packing of circles[33,34].

Definition 4.1. Lattice and lattice packing. A *lattice* in the plane is an infinite set of points such that adding or subtracting any one point to/from another in the lattice returns another point in the lattice, any two points of the lattice are separated by a minimum distance, and any point in the plane is within a maximum distance of a lattice point.

A *lattice packing* is a packing of the plane by congruent geometric objects, such that the centers of the objects are located at the points of a lattice.

Example 4.2. The points in the plane with integer coordinates form a lattice.

Example 4.3. The tiling of the plane by equilateral triangles, squares, or hexagons is a lattice packing. So is the hexagonal circle packing, in which every circle is surrounded by six other circles touching it.

Lemma 4.4. A lattice is invariant under isometries that take one point of the lattice to another point of the lattice.

Lemma 4.5. There are five types of a lattice in the plane (Kittel, 1966, Chapter 1) (**Supplementary Figures 1A – 1E**).

1) Oblique
2) Square
3) Hexagonal
4) Rectangular
5) Centered rectangular

Definition 5. Convexity. A geometric object in the plane is *convex* if for any line segment whose endpoints lie on the object, the entirety of the line segment also lies on the object (**Supplementary Figures 1F – 1H**).

Definition 6. Trajectory. A *trajectory* is a path taken in space.

Definition 7.1. Cell sequence. A *cell sequence* refers to continuous neural activity consisting of sequentially active cells or cell assemblies.

Remark 7.2. In the context of a cell sequence, a "cell" within this sequence refers either to a single cell or a cell assembly. Cell assemblies can perform pattern completion and are thereby resistant to noise so that a cell assembly is activated robustly even if a single cell of this assembly fails to be activated at times.

Definition 8. Sequence coding of trajectories. *Sequence coding of trajectories* is given if the identity of the next active cell in a cell sequence is uniquely determined by the current active cell and the velocity vector associated with the current trajectory (**Figures 1E – 1J**).

Axioms (Table 1). Our goal is to provide a mathematical proof that spatial periodicity in grid cell firing emerges as a parsimonious solution to provide a code for trajectories in 2D space by cell sequences.

The next result shows that if we assume axioms 1 to 4, it must be the case that every firing field of trajectory-coding cells in a computational unit must be congruent (the same shape), and the centers of the firing fields must be arranged in a hexagonal lattice.

Proposition 9.1. Assuming axioms 1 to 4, the firing fields of trajectory-coding cells must be congruent shapes in a hexagonal lattice packing.

Proof 9.2. By Axiom 3, a particular firing field U is surrounded by the maximal number of other firing fields, each of which must be congruent to each other. This implies that every firing field around U is congruent. Since this holds for every firing field U, all firing fields must be congruent. Since each firing field U must be surrounded by the maximal number of firing fields, the kissing number of the arrangement must be maximal. Further, by the symmetry requirement, this must be achieved by a hexagonal lattice packing with a kissing number of 6 (**Figures 1I – 1J**). Any square lattice packing either has a kissing number of 4, or lacks symmetry between the "corner" firing fields and "side" firing fields. □

To visualize the congruence argument above, start with the firing fields that surround a firing field of a trajectory coding cell U. By our axioms, they must all be congruent. Pick one of them, say V, and look at the firing fields around V. Again by our axioms, all the firing fields around V must be congruent. Continue in all directions to see that all firing fields must be congruent.

Lemma 10.1. By axiom 1, the firing fields of trajectory-coding cells must be convex.

Proof 10.2. If some cell has a non-convex firing field, a single cell sequence may code for more than one trajectory (**Supplementary Figure S1H)**. □

In the next result, we show that if we start in a firing field of one trajectory-coding cell and travel in some direction, the sequence of cells that fire must eventually repeat. For example, if cells 1,3, and 4 fire in that order, if an animal continues traveling in the same direction, cells 1,3, and 4 will eventually fire again in that order.

Theorem 11.1. Assuming axioms 1 and 4, the firing fields of trajectory-coding cells must be spatially periodic, in the sense that starting at any point and continuing in a single direction, the initial sequence of locally active cells must eventually repeat with a repeat length of at least 3 (**Figure 2**).

Proof.11.2. Starting in a firing field of cell i and going along any set of firing fields, some cell must eventually become active again since the total number of cells is finite by axiom 4. Once there is a repeat of one cell's firing field, the whole sequence of firing fields of all cells must repeat by axiom 1. This repeating sequence of locally active cells must at least have length 3 as if we had a repeat of length 2, we would have a sequence i, j, i. In this case i, j would represent two distinct trajectories, contradicting axiom 1. □

Remark.11.3. This does not require symmetry in the sense that traveling in two different directions from cell *i* may give repeating sequences of two different lengths, as seen in **Figure 2B**, where the repeats have lengths 4 and 8, depending on the angle of travel from a given cell.

The next goal is to determine how our axioms restrict the arrangement of firing fields in a single computational unit of trajectory-coding cells. Since these firing fields are arranged in a hexagonal lattice, we determine the possible ways to label the firing fields in this lattice (drawn as circles for convenience), as visually representated in Figures 4 and 5.

Many of the proofs in the rest of this section use the method of proof by cases: we describe all possible ways to label the firing fields, and then explain why some of those cases contradict our hypotheses.

Lemma 12.1. Every sequence of cells along one of the three major axes of the hexagonal lattice (from here on referred to as row or diagonal) must be either a translation of an existent sequence in a parallel axis or consist of a disjoint set of cells.

Proof 12.2. Without loss of generality, if row A consists of cells $1, \dots, k$ repeating in this order, then any row that contains any cell from $1, \dots, k$ must contain the full repeat $1, \dots, k$ by axiom 1. So any row containing any cell from $1, \dots, k$ is a translation of row A, and any cell that does not contain them is disjoint from row A. □

Remark 12.3. We will count the distance of a translation of a row A by starting at a cell a, passing to the cell diagonally down and to the right of cell a, and counting spaces moved right from here. Translations must be by $0,1,2, \dots, k-1$ spaces, where row A contains k cells.

Lemma 13.1. If a row or diagonal of the hexagonal lattice is a translation of a neighboring row or diagonal, the translation must be by at least 2 and at most $n-3$, where n is the repeat length.

Proof 13.2. Translating by $0,1,n-2$, or $n-1$ leads to a contradiction of axiom 1. □

Lemma 14.1. Sequence repeats in parallel rows or diagonals must be of the same length.

Proof 14.2. If two consecutive rows have sequence repeats of different lengths, say row A consists of $1,\dots,k$ and row B consists of $k+1,\dots,k+s$, where $k<s$, then $1,k+1$ will appear in one repeat and $1,k+t$ will appear in the next, where t is not equal to 1. This contradicts axiom 1 (**Figure 5A**). □

Lemma 15.1. The length of the sequence repeat in any row or diagonal must divide the number of cells. As a result, if the number n of cells is prime, the length of the sequence repeat in any row or diagonal must be of length n.

Proof 15.2. Suppose the repeat length is less than n in some dimension. Without loss of generality, assume it is the horizontal direction, so that one row consists of $1,2,\dots,i$ repeating, for some $i<n$. Then every row must have repeat length i by Lemma 14.1. Since every row must consist of cells $1,2,\dots,i$ or be disjoint from the cells in other rows by Lemma 12.1, every cell will appear in exactly 1 of the distinct rows, so the length of the repeat in each row must divide n.

If n is prime, every row has repeat length dividing n. Since no row can have a repeat of length 1, every row has repeat length n.

Next, we use the setup above to prove that the minimum number of trajectory-coding cells in a computational unit is 7, and describe the two ways for 7 cells to make up a computational unit.

Theorem 16.1. The minimum number of distinct cells providing a sequence code of trajectories in 2D space is 7, and there are exactly 2 possible arrangements of the cells so that cell sequences code for trajectories in 2D space, up to relabeling of the cells.

Proof.16.2. Given the requirement that each cell has 6 distinct cells around it, the minimum number of cells is 7.

By Lemma 15.1, the repeat length must be 7 in all directions. We may assume without loss of generality that row A consists of cells $1,2,\dots 7$ (**Figure 3B**). Hence, every row is a translation of row A. By Lemma 13.1 and trial and error, there are two options (**Figure 3B**). □

In Table 2, we list all possible ways to construct a computational unit from 7-12 trajectory-coding cells up to translation and rotation.

While solutions with 7 neurons result in a hexagonal lattice packing of firing fields, solutions with 8 or more neurons can result in other types of lattice packing (**Supplementary Figure 1**), such as the oblique lattice or centered rectangular lattice that have also been observed in single unit recordings of freely behaving animals[36]. Code to compute and visualize "grid maps" of trajectory-coding cell

sequence arrangements with up to 14 cells has been made publicly available to help the scientific community test some of our predictions against future datasets[37].

Importantly, the grid pattern that we have found to emerge as the most parsimonious solution assuming axioms 1 to 4 (see Results), i.e., the solution to sequence coding of trajectories with a minimal number of neurons, mirrors experimental results on grid cells from animal experiments as we demonstrate below.

Sequence coding of trajectories predicts grid spacing and rotation of grid maps against a wall

The solution to sequence coding of trajectories predicts firing fields on the single cell level that form a hexagonal lattice, as observed in grid cell data obtained from freely behaving rodents[2,38] and crawling Egyptian fruit bats[39]. The triangular structure of grid cells' firing maps (grid maps) have been characterized by three parameters, namely grid field size, grid spacing, and grid orientation[2]. When using the distance between the centers of two adjacent grid fields to measure grid spacing and a diameter-like metric to measure grid field size, the sequence code of trajectories model of grid cell firing predicts a fixed ratio of grid spacing to field size of $\sqrt{7} \approx 2.65$ (see Methods). We tested this prediction on a data set of n = 27 grid cells recorded in mice for a previously published study[40]. Quantifying field sizes requires identifying the borders of individual fields as a first step. Since the characteristic feature of a firing field is its firing rate, we chose to use a threshold for the firing rate to determine the field boundaries (see Methods). Setting the field detection threshold to 31% of the peak firing rate optimized detection of grid fields in most grid cells (n = 25 out of 27 cells) (**Supplementary Figure S2A**). Note that the grid field size measured from firing rate maps of experimental data is expected to be larger than the model-predicted grid field size, resulting in smaller ratios of grid field spacing to field size, because the model prediction reflects the ideal ratio and does not take into account noise in experimental measurements, transient drifts of grid maps, path integration errors, conjunctive coding properties, or any other factors that result in out-of-field firing of neurons recorded in experiments (**Supplementary Figures S2C and S3**). We found that the ratio of the field spacing to a diameter-like metric of the field size was 2.39 ± 0.25 (mean ± SD; n = 25) (**Supplementary Figure S2B**), consistent with experimental results obtained from mice.

Another testable prediction of our model is that the grid map associated with the most parsimonious solution using seven cells is rotated by 10.9 degrees against the nearest wall of a rectangular enclosure (Table 2). This angle is within the range of experimentally observed values. Concretely, Stensola et al. (2015) reported a distribution of angles with a plateau between ~6 and ~12 degrees (mean ± SD: 7.2 ± 3.5). Notably, the median of the angle to the nearest wall in a highly familiar as opposed to a novel environment was 9.8 degrees[36]. The sequence code model of grid cell firing thus provides a simple and intuitive answer to the otherwise puzzling observation that most grid field maps observed in freely behaving animals are rotated against the nearest wall of a rectangular enclosure.

Sequence coding of trajectories predicts fragmentation of grid maps in 1D space

Another experimental observation related to the spatial geometry of grid fields that can be explained by a sequence code of trajectories is the fragmentation of grid cell maps in a multicompartment

environment (**Figures 4A – 4C**). The two-dimensional spatial periodicity in grid cell firing is replaced by one-dimensional (1D) spatial periodicity if movement through space is restricted to 1D trajectories along parallel alleys in a multi-compartment maze[41]. A sequence code of trajectories predicts such a fragmentation of grid cell maps because parallel trajectories would result in the same sequential activation of cells, and neural coding on a 1D tract is most efficient when sequences are aligned with the movement direction (**Figure 4A**). Likewise, grid cells have been shown to path integrate distances on a 1D circular track[42], consistent with a cell sequence code of a trajectory along a 1D circular track (**Figure 4B**). Notably, Jacob et al. (2019) report in their study that the field spacing of grid cells is increased in a 1D circular track compared to a 2D environment. The authors' explanation is that field spacing is increased due to the lack of visual cues. However, an alternative explanation based on the sequence model of grid cell firing is that running through a cell sequence on a linear track would activate the complete sequence of cells until the sequence repeats itself (**Figure 4C**). Moreover, the cell sequence code of trajectories is consistent with an analysis of experimental data[43] showing that firing fields of grid cells on a 1D linear track are compatible with a slice through a 2D hexagonal pattern. Specifically, a slice through a 2D hexagonal firing pattern explains linear-track data if translational shifts of the pattern are allowed at turning points without a requirement of rotating or scaling the grid. In the context of the sequence code of trajectories, a translational shift of the grid pattern of a single cell is equivalent to re-anchoring the sequence code after the animal has turned around facing the opposite direction on the linear track. Such a translational shift or re-anchoring of the sequence code is consistent with experimental data showing differential spatial coding by place cells in the hippocampus for inbound and outbound running directions on a linear track[44].

Furthermore, grid cells have been shown to code for traveled distance, elapsed time, or a combination of distance and time when animals run in place on a treadmill[45]. The firing pattern of grid cells as time or distance cells is remarkably similar to the firing pattern of grid cells that emerges when animals navigate 1D linear tracks after correcting for logarithmic expansion in grid field size over time. The fact that grid cells show repeating firing fields in other dimensions than physical space is consistent with a sequence code of trajectories in any type of dimension that has behavioral relevance for the animal. Experimental data[45] demonstrate parallel coding of different dimensions by different grid cells, suggesting individual grid cell sequences can provide independent codes of trajectories through different dimensions, thereby enabling parallel processing of different cognitive functions.

Sequence coding of trajectories predicts rescaling and restructuring of grid maps in response to changes in a familiar environment

A cell sequence code of trajectories does not need to be rigid but instead can be malleable and rescaled in response to changes in the environment as long as the start and end points of the sequences are anchored to salient environmental landmarks. Thus, sequence coding of trajectories by grid cells provide an explanation of distortions of the grid pattern that are frequently observed in animal studies. Experiments in freely behaving rodents demonstrate that stretching or compression of enclosed environments result in stretching or compression of the grid map in the rescaled dimension. For instance, stretching or compressing the borders of a familiar open field recording arena resulted in an increase or decrease of the distance between firing fields in the rescaled dimension of the deformed enclosure[36,46]. Such distortions have been challenging to interpret under

the assumption that grid cells provide a “spatial metric” or “coordinate system” for navigation. However, if we assume a cell sequence code with start and end points of trajectories anchored to landmarks or environmental borders, distortions of the grid along the rescaled dimension would be expected. The sequence code of trajectories would remain the same if trajectories are defined relative to the borders of the environment (**Figure 4D**). Moreover, experimental data in rats show that grid maps that have been established in two adjacent compartments separated by a wall within the same larger environment merge once the wall is removed[47]. Merging of the two grid maps appeared to happen instantly resulting in local spatial periodicity and continuity between the two original maps[47], consistent with the sequence code of trajectories by grid cells.

Scaling of grids has also been observed in the form of an expansion, i.e., increased grid spacing between individual firing fields and increased field sizes, in response to novelty of the environment[48]. Such scaling has also been reported in climbing rats foraging on a vertical wall[49]. As the scaling of grids in response to scaling the borders of an environment is inconsistent with the hypothesis that grid cells provide a spatial metric for navigation or path integration, so is an expansion of grid fields in response to novelty. However, an increase in grid spacing in response to a novel environment can be explained by a cell sequence code of trajectories where the distance between the centers of firing fields are initially larger in novel environments reflecting a broader spatial resolution in a trajectory code by neural sequences because the overall layout of the space is more important than the fine-grained details. As the animal becomes more familiar with the environment, it will pay more attention to spatial details and hence uses a trajectory code with higher spatial resolution, resulting in a smaller field size and a smaller grid map. While this hypothesis needs to be tested in future studies, experimental data show that changes in grid field size co-occur, though to a lesser extent, with changes in the size of place cell firing fields in response to novel environments[48,50,51]. In summary, sequence coding of trajectories is consistent with the experimentally observed scaling of grids in response to deformations of the borders of the environment and with compression or expansion of firing fields and grid spacing in response to novelty.

Furthermore, cell sequence coding of trajectories in 2D space provides an explanation of experimental data showing that grid fields move toward goal locations[52] or restructure their spatial firing maps to incorporate the location of a learned reward[53]. These data support the hypothesis that grid cells do not provide a simple metric of space. Instead, the spatial firing pattern of grid cells is malleable in response to relevant contextual features. Such local distortions of global grid patterns by salient locations have recently been compared to spacetime distortions by blackholes[54]. We propose that such warping of grid maps is caused by an increased probability that the currently active grid cell activates the next grid cell in the sequence of trajectory-coding cells. This would result in a progressive decrease in grid spacing that could yield a gradual increase of overlap of grid fields or deformations of grid fields near a goal location, thereby causing local distortions in the grid map of a single grid cell. The result is that grid fields of a single grid cell appear to have moved closer to the goal location (**Figure 4E**). A cell sequence code of trajectories by grid cells is thus consistent with malleable grid maps because the spacing between adjacent firing fields can change gradually in response to local contextual features without compromising the sequence code. The same mechanism can explain shearing induced assymmetry and multiple alignment solutions that have been shown in experimental data[36].

Multiple grid units provide nearly continuous resolution in the coding of trajectories and predict grid cell properties on the population level

In addition to properties of grid cell firing on the single cell level, the definition of sequence coding of trajectories implies an intriguing property of grid cells on the population level, namely that each grid cell's collection of firing fields is geometrically congruent to any other grid cell's collection of firing fields. This property mirrors experimental data from single unit recordings in rodents showing that adjacent firing field grid patterns of different anatomically close grid cells differ only in phase but have the same orientation and scale[2]. Since the firing fields of the seven grid cells of a fundamental grid unit (i) do not overlap and (ii) discretize directions into six running directions only, the questions arise of how other running directions are represented and how smooth transitions between firing fields can be accomplished. Consistent with experimental data[2], the sequence code of trajectories model of grid cell firing accounts for smooth transitions between firing fields and the representations of more than six running directions by using multiple fundamental grid units of seven cells with the same field size and spacing, but whose firing fields are shifted slightly in phase, so that their field centers fall in between two other firing fields (**Figures 5A and 5B**).

Two key conclusions from this theoretical result are that (i) an arbitrarily smooth transition between grid fields/grid cells becomes possible during navigation with an arbitrarily large number of grid cells (organized in fundamental units of seven cells with non-overlapping firing fields), and (ii) traveling directions can be represented with an arbitrarily high angular resolution (see also the **video animation** of the sequence model associated with this study). This is consistent with experimental data on simultaneously recorded multiple grid cells with overlapping firing fields and consistent with data showing that grid cell dynamics can be represented with a toroidal manifold (**Figure 5C**).

Moreover, experimental data have shown that grid cells cluster into autonomous modules with distinct scale, orientation, symmetry and theta frequency modulation[55]. If we assume that grid cells emerge from a cell sequence code of spatial trajectories, adjacent firing fields in that sequence would provide a discrete sequence of sampling points in the coding of trajectories, and the distance between the centers of two adjacent firing fields would determine the spatial resolution. Doubling the number of sampling points, i.e., doubling the number of firing fields per unit area would double the spatial resolution[56]. Conversely, dividing the number of firing fields per unit area in half would halve the spatial resolution. To double or halve the spatial resolution in 2D space, the number of firing fields per area needs to double or be cut in half, respectively (**Supplementary Figure S4**). Because firing fields are densely packed, doubling the number of firing fields per unit area in 2D space would result in dividing the distance between two adjacent firing fields by a factor of $\sqrt{2}$. This is exactly what has been observed in animal experiments[36].

DISCUSSION

A teleological cause for the existence of grid cells

In this study, we prove mathematically that spatial periodicity in grid cell firing emerges as the only possible solution to provide a code of trajectories in 2D space by cell sequences. Within the space of all possible solutions, hexagonal symmetry in grid cell firing emerges as the most parsimonious solution. The hexagonal firing pattern of grid cells in 2D space is arguably their most intriguing

property. Yet, despite decades of experimental and theoretical research, the fundamental nature of the computational problem solved by grid cells has remained largely elusive. Previous studies on grid cells have been fruitful in describing functional properties of grid cells and grid cell firing at the level of neuroanatomy, connectivity, neurophysiology, and circuit dynamics, but have largely failed to provide a specific and intuitive answer to why grid cells have evolved: what is the computational advantage of grid cells over other potential mechanisms or algorithmic implementations in the context of a computational goal? Previous investigations of grid cell function[22–24] based on mechanistic models such as the oscillatory interference[15–19] or continuous attractor models[4,20,21] do not address the computational goal of or teleological cause for the existence of grid cells. Other studies have used normative models to demonstrate that grid patterns can emerge to optimize the coding of space by grid cells[57,58] or to optimize path integration[32,59,60]. However, these normative models fall short in demonstrating that grid cells are necessary as opposed to providing an optimal solution for the assumed normative functions and often rely on hidden architectural, hyperparameter, and constraint choices to obtain grid cell firing patterns[61] as discussed under the next section "Normative models of grid cell firing".

We therefore deviated from these traditional approaches of investigating the nature of grid cell properties and asked the question: Is there a brain function that could either not be performed at all or would be substantially more costly or difficult to perform in the absence of grid cells? To constrain our search for such a function, we assumed that any coding mechanisms that operates on spatial firing requires cell sequences as a fundamental neural syntax in the brain[27–29]. Assuming that neural coding of trajectories in 2D space is important for animal navigation, we show that grid cells are the most effective solution. We demonstrate that 7 neurons are sufficient to provide an unambiguous code for trajectories in 2D space and that the only two possible solutions with 7 neurons result in firing fields that fall on a hexagonal grid. Notably, these two solutions result in grid maps that are mirror images of each other up to relabeling the cells. Any other solution to the problem would require at least 8 neurons, an increase in the number of neurons forming a grid unit by more than 14%. Note that an increase in the number of neurons within one grid unit would not result in an increase in spatial or angular resolution in the coding of trajectories. It can therefore be reasoned that performing the same computational function with the minimum number of neurons forming a grid unit is evolutionary advantageous because it conserves space, cellular material, energy, and resources[62]. A solution to a sequence code of trajectories that builds on fundamental units of only 7 grid cells compared to a larger number of cells would then be expected to be most frequently adopted. We therefore argue that we have provided a teleological cause for the existence of grid cells and an answer to the fundamental question of why grid cells have emerged in brains of navigating animals, namely that grid cells are the most parsimonious solution to sequence coding of trajectories in 2D space.

Normative models of grid cell firing

Normative models generally fall into two classes: One that uses artificial neural network models and one that uses a mathematical or analytical approach. Grid-like firing has been found to emerge in artificial neural networks when the models were trained to perform path integration under simple biologically plausible constraints. The emerged grid cells then endowed agents with the ability to perform vector-based navigation[32,59]. While these models demonstrate that path integration is an important driving force in the generation of grid cells, the mechanism that is generating grid cell

firing patterns remains obscure due to the untransparent nature of neural networks. Moreover, the results often depend on specific hyperparameter choices to explain the emergence of grid-like units under anatomical constraints (see[61] for a discussion). In contrast, we have provided mathematical proof here that the emergence of lattice packings of firing fields is implied by a cell sequence code of trajectories in 2D space, and that the most parsimonious solution uses only seven cells in one grid unit.

Recently, a normative model by Dorrell et al. (2023) has introduced the concept of "actionable representations", which is similar to what we have called a code of trajectories in our study. The authors of that study formulate actionable representations using group and representation theory, and show that, when combined with biological and functional constraints, multiple modules of hexagonal grid cells are the optimal representation of 2D space. In contrast, our study does not focus on explaining an optimal representation of space but instead focuses on demonstrating that spatial periodicity emerges from a neural sequence code of trajectories. In our framework, spatial periodicity in grid cell firing emerges as a by-product of a path-integration function, and spatial periodicity has no function in optimizing coding of space. However, we demonstrate in Supplementary Figure S2 that the spacing observed across different grid cell modules is consistent with optimizing spatial resolution in trajectory coding. The mathematical proof presented in this study does not require any assumptions about mechanistic implementations of the code of trajectories by cell sequences. Any implementation that aims at providing a code for trajectories by cell sequences in a 2D space must result in a lattice packing of firing fields, and minimizing the required number of cells in that code results in a hexagonal lattice of the firing fields of a single cell. In artificial systems, other lattice configurations are possible, though significantly less computationally efficient. Therefore, we identified a teleological cause for the emergence of grid cells in the brain of navigating animals.

Sequence coding of trajectories by grid cells provides a mechanistic explanation for how grid cells serve path integration and can support memory-guided navigation

If the step-by-step advancements from the currently active cell to the next cell in the grid cell sequence are caused by integrating velocity signals, grid cells perform path integration. The ensuing grid cell sequence is then the result of the path integration and can be interpreted as a sequence code by a downstream reader, potentially the hippocampus. Different grid cell modules integrate velocity signals at different (spatial) scales that are determined by the distance between the grid field centers of adjacent cells in the sequence. A sequence code of trajectories by grid cells therefore provides a mechanistic explanation for the functional role of grid cells in path integration. The model described in this paper can be implemented with temporal coding (spiking neurons) or rate coding, or even with binary activity states of neurons, where neurons are activated sequentially as a function of the animal's velocity. Previous modeling work has shown that circuit mechanisms using grid cells in combination with speed-modulated head direction cells and hippocampal place cells can provide a substrate for episodic encoding and retrieval of spatiotemporal trajectories[7]. Furthermore, grid cell sequences have been shown to be useful in simulations of new goal-directed trajectories, where grid cells were used in a network of head direction cells, hippocampal place cells and persistent spiking cells to plan forward trajectories through the environment that search for place cells near a goal location[14]. Recent experimental data demonstrate that temporally coordinated entorhinal inputs

drive hippocampal sequences to perform memory-guided navigation[26] and that temporally structured population activity of grid and place cells represent local trajectories essential for goal-directed navigation and planning[63].

It would provide an advantage to animals if they could plan trajectories towards goals on different spatial scales to "zoom in" or "zoom out" on a cogntive map of their environment. We therefore proposed that each grid module represents trajectories at progressively lower or higher resolution to enable planning of trajectories across different spatial scales. This approach is analogous to mip mapping known from computer graphics, where an image is sampled by a stack of images, each of which is represented with half the resolution of the previous to increase rendering performance[56]. Notably, in a 1D environment, doubling the number of firing fields per unit length would result in dividing the distance between two adjacent firing fields in half. It remains to be tested experimentally whether grid cell modules can adapt the scaling factor to optimize computational efficiency in multiscale representation of 1D environments.

The grid cell model presented in this study assumes the ideal tiling of space and equal representation of traveling direction. If this assumption was relaxed, there would be gaps in the representation of space and traveling direction or some traveling directions will be represented with larger or smaller fields, hence with smaller or larger angular resolution, respectively (see **Figures 1I – 1J**). However, path integration performed by animals is far from being perfect, and it would be of interest for future work to investigate whether non-ideal tiling of space by grid cells may be one of many factors contributing to errors in path integration[30,31]. One potential mechanism to compensate for non-ideal tiling of space is population coding. Grid cells can be part of grid cell assemblies, and the population activity of many multiple grid units consisting of seven grid cell assemblies can be interpreted by a reader mechanism as a robust population code.

Notably, sequence coding of trajectories is not limited to physical space but could be useful for cognitive functions such as working memory or episodic memory that connects events into a cohesive story, consistent with experimental data demonstrating a grid-like code of conceptual knowledge space in humans[10]. A sequence code of trajectories by grid cells can thus explain data from human subjects that link reduced grid-like activity with path integration deficits observed in Alzheimer's disease risk carriers[64,65], and data from rodent experiments demonstrating that grid cell firing is reduced in a rodent animal model of Alzheimer's disease[66,67].

Sequence coding of trajectories in 3D space

There is no reason to assume that the sequence code of trajectories described in this study is restricted to 2D space. We have discussed in previous paragraphs how a sequence code of trajectories by grid cells can code for trajectories in 1D space. In principle, such a sequence code can be expanded to three-dimensional (3D) or higher dimensional spaces. However, there are multiple equally optimal possibilities to generate a close-packed arrangement of firing fields in 3D space[68,69], where each sphere touches 12 neighboring spheres. Two examples of lattice packings in 3D that achieve this kissing number are the face-centered cubic and hexagonal close packed arrangements, which both have layers arranged in hexagonal lattices but stack the layers differently[70]. A model based on a sequence code of trajectories by grid cells would therefore predict larger variability in spatial periodicity of grid cell firing in 3D space compared to 2D space. It

remains to be determined whether specific solutions to cell sequence coding of trajectories in 3D space could result in local or global symmetries. The distribution of grid cell firing fields in rats exploring a 3D volumetric space is irregular[71]. However, since sequences need to repeat, cell sequence coding of trajectories in 3D space predicts some degree of local order in the grid map of a single grid cell. Consistent with this prediction, experimental data show that grid cells recorded in flying bats exhibit fixed local distances between firing fields despite the lack of a global lattice arrangement of firing fields[72]. Taken together, these experimental data are consistent with a sequence code of trajectories that expands to 3D space, even though this sequence coding may not need to result in a globally symmetric arrangement of the firing fields of a single cell. Based on data from animals navigating in 3D environments, it has recently been proposed that the characteristic hexagonal firing pattern of grid cells is a "by-product of whatever process causes the cells to fire in spatially discrete regions of uniform size."[73] This study demonstrates that said process is a neural sequence code of trajectories.

Limitations of the study

This study demonstrates a teleological cause for the existence of grid cells, namely sequence coding of trajectories in 2D. The goal of this study was thus not to provide a mechanistic model of grid cells or biologically-detailed model of the connections between neurons that can mechanistically account for grid cell firing. The model thus remains agnostic about the specific mechanistic implementation as to how a velocity signal is integrated in entorhinal circuits to move activity from one neuron in the sequence to the next neuron in the sequence as a function of the animal's velocity and makes no predictions about connectivity between neuron types and the connenction strengths.

While we have demonstrated that the ratio of grid field spacing to grid field size in an experimental data set of grid cells obtained from mice is consistent with the prediction made by the trajectory code by neural sequences model of grid cell firing, we acknowledge that future studies should test this model prediction on larger data sets of grid cells obtained from species other than mice and recorded from different grid cell modules.

Acknowledgments

This work was supported by the National Institute of Neurological Disorders and Stroke of the National Institutes of Health, grant numbers R00NS116129 to H.D. and R01NS39600 to G.A.A. Thank you to Harrison Bray for helpful conversations about lattice packings, and thank you to Xihui Zheng for help with graphical illustrations. We thank Michael E. Hasselmo for sharing data with us and for comments on the manuscript. We thank Marc W. Howard for helpful comments on the manuscript.

References

1. Fyhn, M., Molden, S., Witter, M.P., Moser, E.I., and Moser, M.-B. (2004). Spatial representation in the entorhinal cortex. Science *305*, 1258–1264. http://dx.doi.org/10.1126/science.1099901.

2. Hafting, T., Fyhn, M., Molden, S., Moser, M.-B., and Moser, E.I. (2005). Microstructure of a spatial map in the entorhinal cortex. Nature *436*, 801–806. http://dx.doi.org/10.1038/nature03721.

3. Boccara, C.N., Sargolini, F., Thoresen, V.H., Solstad, T., Witter, M.P., Moser, E.I., and Moser, M.-B. (2010). Grid cells in pre- and parasubiculum. Nat. Neurosci. *13*, 987–994. 10.1038/nn.2602.

4. Fuhs, M.C., and Touretzky, D.S. (2006). A spin glass model of path integration in rat medial entorhinal cortex. J. Neurosci. Off. J. Soc. Neurosci. *26*, 4266–4276. 10.1523/JNEUROSCI.4353-05.2006.

5. McNaughton, B.L., Battaglia, F.P., Jensen, O., Moser, E.I., and Moser, M.-B. (2006). Path integration and the neural basis of the "cognitive map". Nat Rev Neurosci *7*, 663–678. http://dx.doi.org/10.1038/nrn1932.

6. Moser, E.I., Moser, M.-B., and McNaughton, B.L. (2017). Spatial representation in the hippocampal formation: a history. Nat. Neurosci. *20*, 1448–1464. 10.1038/nn.4653.

7. Hasselmo, M.E. (2009). A model of episodic memory: mental time travel along encoded trajectories using grid cells. Neurobiol. Learn. Mem. *92*, 559–573. 10.1016/j.nlm.2009.07.005.

8. Eichenbaum, H., and Cohen, N.J. (2014). Can we reconcile the declarative memory and spatial navigation views on hippocampal function? Neuron *83*, 764–770. 10.1016/j.neuron.2014.07.032.

9. Schiller, D., Eichenbaum, H., Buffalo, E.A., Davachi, L., Foster, D.J., Leutgeb, S., and Ranganath, C. (2015). Memory and Space: Towards an Understanding of the Cognitive Map. J. Neurosci. Off. J. Soc. Neurosci. *35*, 13904–13911. 10.1523/JNEUROSCI.2618-15.2015.

10. Constantinescu, A.O., O'Reilly, J.X., and Behrens, T.E.J. (2016). Organizing conceptual knowledge in humans with a gridlike code. Science *352*, 1464–1468. 10.1126/science.aaf0941.

11. Hawkins, J., Lewis, M., Klukas, M., Purdy, S., and Ahmad, S. (2018). A Framework for Intelligence and Cortical Function Based on Grid Cells in the Neocortex. Front. Neural Circuits *12*, 121. 10.3389/fncir.2018.00121.

12. Rueckemann, J.W., Sosa, M., Giocomo, L.M., and Buffalo, E.A. (2021). The grid code for ordered experience. Nat. Rev. Neurosci. *22*, 637–649. 10.1038/s41583-021-00499-9.

13. Bush, D., Barry, C., Manson, D., and Burgess, N. (2015). Using Grid Cells for Navigation. Neuron *87*, 507–520. 10.1016/j.neuron.2015.07.006.

14. Erdem, U.M., and Hasselmo, M.E. (2014). A biologically inspired hierarchical goal directed navigation model. J. Physiol. Paris *108*, 28–37. 10.1016/j.jphysparis.2013.07.002.

15. O'Keefe, J., and Burgess, N. (2005). Dual phase and rate coding in hippocampal place cells: theoretical significance and relationship to entorhinal grid cells. Hippocampus *15*, 853–866. 10.1002/hipo.20115.

16. Burgess, N., Barry, C., and O'Keefe, J. (2007). An oscillatory interference model of grid cell firing. Hippocampus *17*, 801–812. 10.1002/hipo.20327.

17. Giocomo, L.M., Zilli, E.A., Fransén, E., and Hasselmo, M.E. (2007). Temporal frequency of subthreshold oscillations scales with entorhinal grid cell field spacing. Science *315*, 1719–1722. 10.1126/science.1139207.

18. Hasselmo, M.E., Giocomo, L.M., and Zilli, E.A. (2007). Grid cell firing may arise from interference of theta frequency membrane potential oscillations in single neurons. Hippocampus *17*, 1252–1271. 10.1002/hipo.20374.

19. Burgess, N. (2008). Grid cells and theta as oscillatory interference: theory and predictions. Hippocampus *18*, 1157–1174. 10.1002/hipo.20518.

20. Burak, Y., and Fiete, I.R. (2009). Accurate path integration in continuous attractor network models of grid cells. PLoS Comput. Biol. *5*, e1000291. 10.1371/journal.pcbi.1000291.

21. Shipston-Sharman, O., Solanka, L., and Nolan, M.F. (2016). Continuous attractor network models of grid cell firing based on excitatory-inhibitory interactions. J. Physiol. *594*, 6547–6557. 10.1113/JP270630.

22. Zilli, E.A. (2012). Models of grid cell spatial firing published 2005-2011. Front. Neural Circuits *6*, 16. 10.3389/fncir.2012.00016.

23. Couey, J.J., Witoelar, A., Zhang, S.-J., Zheng, K., Ye, J., Dunn, B., Czajkowski, R., Moser, M.-B., Moser, E.I., Roudi, Y., et al. (2013). Recurrent inhibitory circuitry as a mechanism for grid formation. Nat. Neurosci. *16*, 318–324. 10.1038/nn.3310.

24. Zutshi, I., Fu, M.L., Lilascharoen, V., Leutgeb, J.K., Lim, B.K., and Leutgeb, S. (2018). Recurrent circuits within medial entorhinal cortex superficial layers support grid cell firing. Nat. Commun. *9*, 3701. 10.1038/s41467-018-06104-5.

25. Marr, D. (2010). Vision: a computational investigation into the human representation and processing of visual information (MIT Press).

26. Liu, C., Todorova, R., Tang, W., Oliva, A., and Fernandez-Ruiz, A. (2023). Associative and predictive hippocampal codes support memory-guided behaviors. Science *382*, eadi8237. 10.1126/science.adi8237.

27. Buzsáki, G. (2010). Neural syntax: cell assemblies, synapsembles, and readers. Neuron *68*, 362–385. 10.1016/j.neuron.2010.09.023.

28. Buzsáki, G., McKenzie, S., and Davachi, L. (2022). Neurophysiology of Remembering. Annu. Rev. Psychol. *73*, null. 10.1146/annurev-psych-021721-110002.

29. Zutshi, I., Leutgeb, J.K., and Leutgeb, S. (2017). Theta sequences of grid cell populations can provide a movement-direction signal. Curr. Opin. Behav. Sci. *17*, 147–154. 10.1016/j.cobeha.2017.08.012.

30. Allen, K., Gil, M., Resnik, E., Toader, O., Seeburg, P., and Monyer, H. (2014). Impaired path integration and grid cell spatial periodicity in mice lacking GluA1-containing AMPA receptors. J. Neurosci. Off. J. Soc. Neurosci. *34*, 6245–6259. 10.1523/JNEUROSCI.4330-13.2014.

31. Gil, M., Ancau, M., Schlesiger, M.I., Neitz, A., Allen, K., De Marco, R.J., and Monyer, H. (2018). Impaired path integration in mice with disrupted grid cell firing. Nat. Neurosci. *21*, 81–91. 10.1038/s41593-017-0039-3.

32. Sorscher, B., Mel, G.C., Ocko, S.A., Giocomo, L.M., and Ganguli, S. (2023). A unified theory for the computational and mechanistic origins of grid cells. Neuron *111*, 121-137.e13. 10.1016/j.neuron.2022.10.003.

33. Thue, A. (1910). Über die dichteste Zusammenstellung von kongruenten Kreisen in einer Ebene. Norske Vid. Selsk. Skr. *1*, 1–9.

34. Tóth, L.F. (1942). Über die dichteste Kugellagerung. Math. Z. *48*, 676–684. 10.1007/BF01180035.

35. Kittel, C. (1966). Introduction to solid state physics 3rd ed. (Wiley).

36. Stensola, T., Stensola, H., Moser, M.-B., and Moser, E.I. (2015). Shearing-induced asymmetry in entorhinal grid cells. Nature *518*, 207–212. 10.1038/nature14151.

37. Gleeson, P., Davison, A.P., Silver, R.A., and Ascoli, G.A. (2017). A Commitment to Open Source in Neuroscience. Neuron *96*, 964–965. 10.1016/j.neuron.2017.10.013.

38. Fyhn, M., Hafting, T., Witter, M.P., Moser, E.I., and Moser, M.-B. (2008). Grid cells in mice. Hippocampus *18*, 1230–1238. http://dx.doi.org/10.1002/hipo.20472.

39. Yartsev, M.M., Witter, M.P., and Ulanovsky, N. (2011). Grid cells without theta oscillations in the entorhinal cortex of bats. Nature *479*, 103–107. 10.1038/nature10583.

40. Dannenberg, H., Lazaro, H., Nambiar, P., Hoyland, A., and Hasselmo, M.E. (2020). Effects of visual inputs on neural dynamics for coding of location and running speed in medial entorhinal cortex. eLife *9*, e62500. 10.7554/eLife.62500.

41. Derdikman, D., Whitlock, J.R., Tsao, A., Fyhn, M., Hafting, T., Moser, M.-B., and Moser, E.I. (2009). Fragmentation of grid cell maps in a multicompartment environment. Nat Neurosci. http://dx.doi.org/10.1038/nn.2396.

42. Jacob, P.-Y., Capitano, F., Poucet, B., Save, E., and Sargolini, F. (2019). Path integration maintains spatial periodicity of grid cell firing in a 1D circular track. Nat. Commun. *10*, 1–13. 10.1038/s41467-019-08795-w.

43. Pröll, M., Häusler, S., and Herz, A.V.M. (2018). Grid-cell activity on linear tracks indicates purely translational remapping of 2D firing patterns at movement turning points. J. Neurosci. Off. J. Soc. Neurosci. 10.1523/JNEUROSCI.0413-18.2018.

44. Dombeck, D.A., Harvey, C.D., Tian, L., Looger, L.L., and Tank, D.W. (2010). Functional imaging of hippocampal place cells at cellular resolution during virtual navigation. Nat. Neurosci. *13*, 1433–1440. 10.1038/nn.2648.

45. Kraus, B.J., Brandon, M.P., Robinson, R.J., Connerney, M.A., Hasselmo, M.E., and Eichenbaum, H. (2015). During Running in Place, Grid Cells Integrate Elapsed Time and Distance Run. Neuron *88*, 578–589. 10.1016/j.neuron.2015.09.031.

46. Barry, C., Hayman, R., Burgess, N., and Jeffery, K.J. (2007). Experience-dependent rescaling of entorhinal grids. Nat. Neurosci. *10*, 682–684. 10.1038/nn1905.

47. Wernle, T., Waaga, T., Mørreaunet, M., Treves, A., Moser, M.-B., and Moser, E.I. (2018). Integration of grid maps in merged environments. Nat. Neurosci. *21*, 92–101. 10.1038/s41593-017-0036-6.

48. Barry, C., Ginzberg, L.L., O'Keefe, J., and Burgess, N. (2012). Grid cell firing patterns signal environmental novelty by expansion. Proc. Natl. Acad. Sci. U. S. A. *109*, 17687–17692. 10.1073/pnas.1209918109.

49. Casali, G., Bush, D., and Jeffery, K. (2019). Altered neural odometry in the vertical dimension. Proc. Natl. Acad. Sci., 201811867. 10.1073/pnas.1811867116.

50. Wilson, M.A., and McNaughton, B.L. (1993). Dynamics of the hippocampal ensemble code for space. Science *261*, 1055–1058. 10.1126/science.8351520.

51. Karlsson, M.P., and Frank, L.M. (2008). Network dynamics underlying the formation of sparse, informative representations in the hippocampus. J. Neurosci. Off. J. Soc. Neurosci. *28*, 14271–14281. 10.1523/JNEUROSCI.4261-08.2008.

52. Boccara, C.N., Nardin, M., Stella, F., O'Neill, J., and Csicsvari, J. (2019). The entorhinal cognitive map is attracted to goals. Science *363*, 1443–1447. 10.1126/science.aav4837.

53. Butler, W.N., Hardcastle, K., and Giocomo, L.M. (2019). Remembered reward locations restructure entorhinal spatial maps. Science *363*, 1447–1452. 10.1126/science.aav5297.

54. Ginosar, G., Aljadeff, J., Las, L., Derdikman, D., and Ulanovsky, N. (2023). Are grid cells used for navigation? On local metrics, subjective spaces, and black holes. Neuron *111*, 1858–1875. 10.1016/j.neuron.2023.03.027.

55. Stensola, H., Stensola, T., Solstad, T., Frøland, K., Moser, M.-B., and Moser, E.I. (2012). The entorhinal grid map is discretized. Nature *492*, 72–78. 10.1038/nature11649.

56. Williams, L. (1983). Pyramidal parametrics. Proc. 10th Annu. Conf. Comput. Graph. Interact. Tech. 10.1145/800059.

57. Mathis, A., Stemmler, M.B., and Herz, A.V. (2015). Probable nature of higher-dimensional symmetries underlying mammalian grid-cell activity patterns. eLife *4*. 10.7554/eLife.05979.

58. Wei, X.-X., Prentice, J., and Balasubramanian, V. (2015). A principle of economy predicts the functional architecture of grid cells. eLife *4*, e08362. 10.7554/eLife.08362.

59. Banino, A., Barry, C., Uria, B., Blundell, C., Lillicrap, T., Mirowski, P., Pritzel, A., Chadwick, M.J., Degris, T., Modayil, J., et al. (2018). Vector-based navigation using grid-like representations in artificial agents. Nature *557*, 429–433. 10.1038/s41586-018-0102-6.

60. Cueva, C.J., and Wei, X.-X. (2018). Emergence of grid-like representations by training recurrent neural networks to perform spatial localization. Preprint at arXiv, 10.48550/arXiv.1803.07770 10.48550/arXiv.1803.07770.

61. Rylan Schaeffer, Mikail Khona, and Ila Rani Fiete (2022). No Free Lunch from Deep Learning in Neuroscience: A Case Study through Models of the Entorhinal-Hippocampal Circuit. bioRxiv, 2022.08.07.503109. 10.1101/2022.08.07.503109.

62. Laughlin, S.B., and Sejnowski, T.J. (2003). Communication in Neuronal Networks. Science *301*, 1870–1874. 10.1126/science.1089662.

63. Chaudhuri-Vayalambrone, P., Rule, M.E., Bauza, M., Krstulovic, M., Kerekes, P., Burton, S., O'Leary, T., and Krupic, J. (2023). Simultaneous representation of multiple time horizons by entorhinal grid cells and CA1 place cells. Cell Rep. *42*, 112716. 10.1016/j.celrep.2023.112716.

64. Kunz, L., Schröder, T.N., Lee, H., Montag, C., Lachmann, B., Sariyska, R., Reuter, M., Stirnberg, R., Stöcker, T., Messing-Floeter, P.C., et al. (2015). Reduced grid-cell-like representations in adults at genetic risk for Alzheimer's disease. Science *350*, 430–433. 10.1126/science.aac8128.

65. Bierbrauer, A., Kunz, L., Gomes, C.A., Luhmann, M., Deuker, L., Getzmann, S., Wascher, E., Gajewski, P.D., Hengstler, J.G., Fernandez-Alvarez, M., et al. (2020). Unmasking selective path integration deficits in Alzheimer's disease risk carriers. Sci. Adv. *6*, eaba1394. 10.1126/sciadv.aba1394.

66. Ying, J., Keinath, A.T., Lavoie, R., Vigneault, E., El Mestikawy, S., and Brandon, M.P. (2022). Disruption of the grid cell network in a mouse model of early Alzheimer's disease. Nat. Commun. *13*, 886. 10.1038/s41467-022-28551-x.

67. Ying, J., Reboreda, A., Yoshida, M., and Brandon, M.P. (2023). Grid cell disruption in a mouse model of early Alzheimer's disease reflects reduced integration of self-motion cues. Curr. Biol. CB, S0960-9822(23)00547-X. 10.1016/j.cub.2023.04.065.

68. Stella, F., and Treves, A. (2015). The self-organization of grid cells in 3D. eLife *4*, e05913. 10.7554/eLife.05913.

69. Weisstein, E.W. Sphere Packing. https://mathworld.wolfram.com/.

70. Conway, J.H., and Sloane, N.J.A. (1999). Sphere packings, lattices, and groups 3rd ed. (Springer).

71. Grieves, R.M., Jedidi-Ayoub, S., Mishchanchuk, K., Liu, A., Renaudineau, S., Duvelle, É., and Jeffery, K.J. (2021). Irregular distribution of grid cell firing fields in rats exploring a 3D volumetric space. Nat. Neurosci. *24*, 1567–1573. 10.1038/s41593-021-00907-4.

72. Ginosar, G., Aljadeff, J., Burak, Y., Sompolinsky, H., Las, L., and Ulanovsky, N. (2021). Locally ordered representation of 3D space in the entorhinal cortex. Nature *596*, 404–409. 10.1038/s41586-021-03783-x.

73. Jeffery, K.J. (2023). Symmetries and asymmetries in the neural encoding of 3D space. Philos. Trans. R. Soc. Lond. B. Biol. Sci. *378*, 20210452. 10.1098/rstb.2021.0452.

74. Dannenberg, H., Kelley, C., Hoyland, A., Monaghan, C.K., and Hasselmo, M.E. (2019). The Firing Rate Speed Code of Entorhinal Speed Cells Differs across Behaviorally Relevant Time Scales and Does Not Depend on Medial Septum Inputs. J. Neurosci. *39*, 3434–3453. 10.1523/JNEUROSCI.1450-18.2019.

75. Sargolini, F., Fyhn, M., Hafting, T., McNaughton, B.L., Witter, M.P., Moser, M.-B., and Moser, E.I. (2006). Conjunctive representation of position, direction, and velocity in entorhinal cortex. Science *312*, 758–762. 10.1126/science.1125572.

76. Gatome, C.W., Slomianka, L., Lipp, H.P., and Amrein, I. (2010). Number estimates of neuronal phenotypes in layer II of the medial entorhinal cortex of rat and mouse. Neuroscience *170*, 156–165. 10.1016/j.neuroscience.2010.06.048.

FIGURES

Figure 1

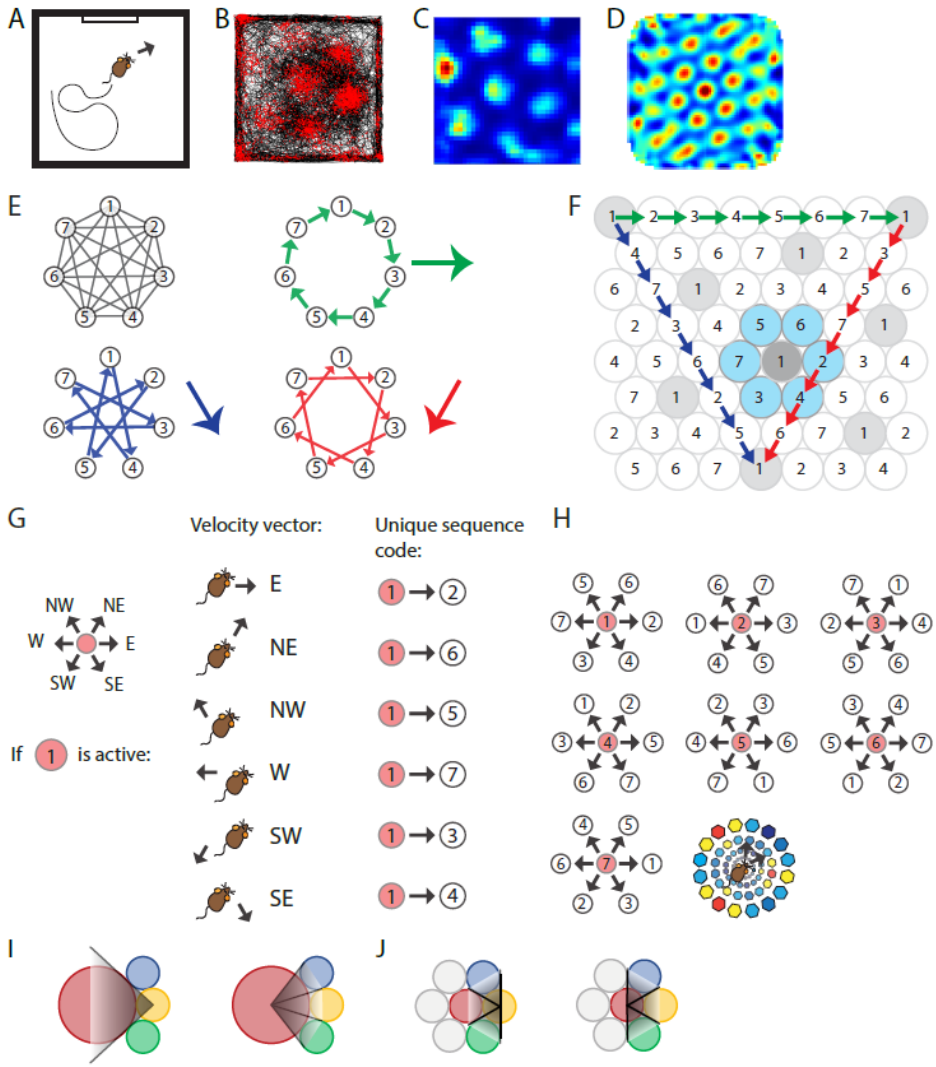

Figure 1. Spatially periodic firing of grid cells in 2D space emerges from a neural sequence code of trajectories. A, Schematic drawing of a 1 x 1 m^2 environment surrounded by walls in the presence of a single visual cue card**. B,** Trajectory plot visualizing grid cell spiking activity as a function of the animal's location in space. Data obtained from the medial entorhinal cortex of a freely foraging mouse [40,74]. The black line indicates the path taken by the animal. Red dots indicate the locations where action potentials (spikes) were generated by the grid cell. **C,** Firing rate map of the spiking data shown in A. Data are visualized as 3 x 3 cm^2 spatial bins, smoothed with a Gaussian kernel. Red and blue colors indicate high and low firing rates. Peak and average firing rates are 15 and 1.9 Hz. **D,** Spatial autocorrelogram of the data shown in B. Red and blue colors indicate high and low correlation values. **E,** Sequential activation map of a fundamental grid unit comprised of seven cells. The sequence of activation is a function of the traveling direction. **F,** The same sequential activation map with seven cells (highlighted in blue) as shown in E but plotted in 2D space with dense packing of firing fields. The firing fields of a single cell form a hexagonal lattice in 2D space, as highlighted for cell #1. **G,** The animal's current velocity vector determines the animal's future trajectory. If the sequence code shall represent as many directions as possible with equal angular resolution from any given starting location, pairs of sequentially active cells need to represent six directions, e.g., North (N), Northeast (NE), Northwest (NW), West (W), Southwest (SW), and Southeast (SE). The current trajectory can be coded by pairs of sequentially active cells. The next active cell in the

sequence is uniquely determined by the current active cell and the velocity vector of the animal (Definition 8). **H,** All possible pairs of cells in the sequence code shown in E and F for the case that the current active cell is cell #1. **I,** Equal angular resolution of movement directions in trajectory coding by cell sequences requires a dense packing of firing fields, i.e., a hexagonal lattice. If a given firing field was surrounded by fewer or more than six firing fields that touched each other, opposite directions would be represented with unequal resolution. **I,** In this example, moving from *east* → *west* cannot be distinguished from the directions *east* → *northwest* and *east* → *southwest* because they are represented by the same cell sequence *yellow* → *red*. However, the opposite direction, *west* → *east*, is represented by three different cell sequences allowing for a finer angular resolution in the representation of traveling direction. **J**, Congruent firing fields that surround each other symmetrically in a hexagonal lattice packing allow for equal angular resolution in the coding of trajectories by cell sequences.

Figure 2

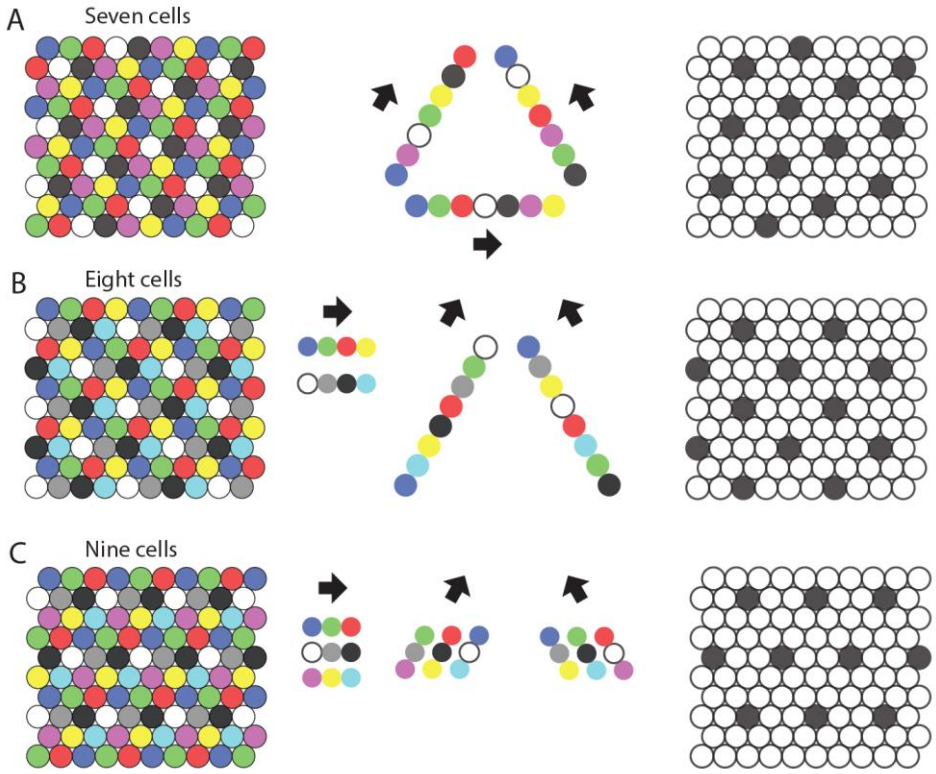

Figure 2. Repeating sequences of cells coding for trajectories result in lattice packing of firing fields. Left panels show firing fields of multiple cells in lattice packings that provide solutions to trajectory coding by cell sequences in 2D space. Mid panels show the cell sequences that code for the three major axes of direction in a dense packing of firing fields. Right panels highlight the firing fields of a single cell to visualize the lattice type formed by the firing fields. **A**, An example of seven cells and sequences with repeat length 7 along all three axes of direction. The resulting firing fields of single cells are arranged on a hexagonal lattice rotated by 10.9 degrees against one wall. This example only needs the minimum number of 7 cells to form unambiguous sequence codes of trajectories. **B**, An example of eight cells and sequences with repeat lengths 4 along one axis, and repeat length 8 along the two other axes of direction. The resulting firing fields are arranged on a centered rectangular lattice. **C**, An example of nine cells and sequences with repeat length 3 along all three axes of direction. The result is a symmetical grid (hexagonal lattice packing) of firing fields.

Figure 3

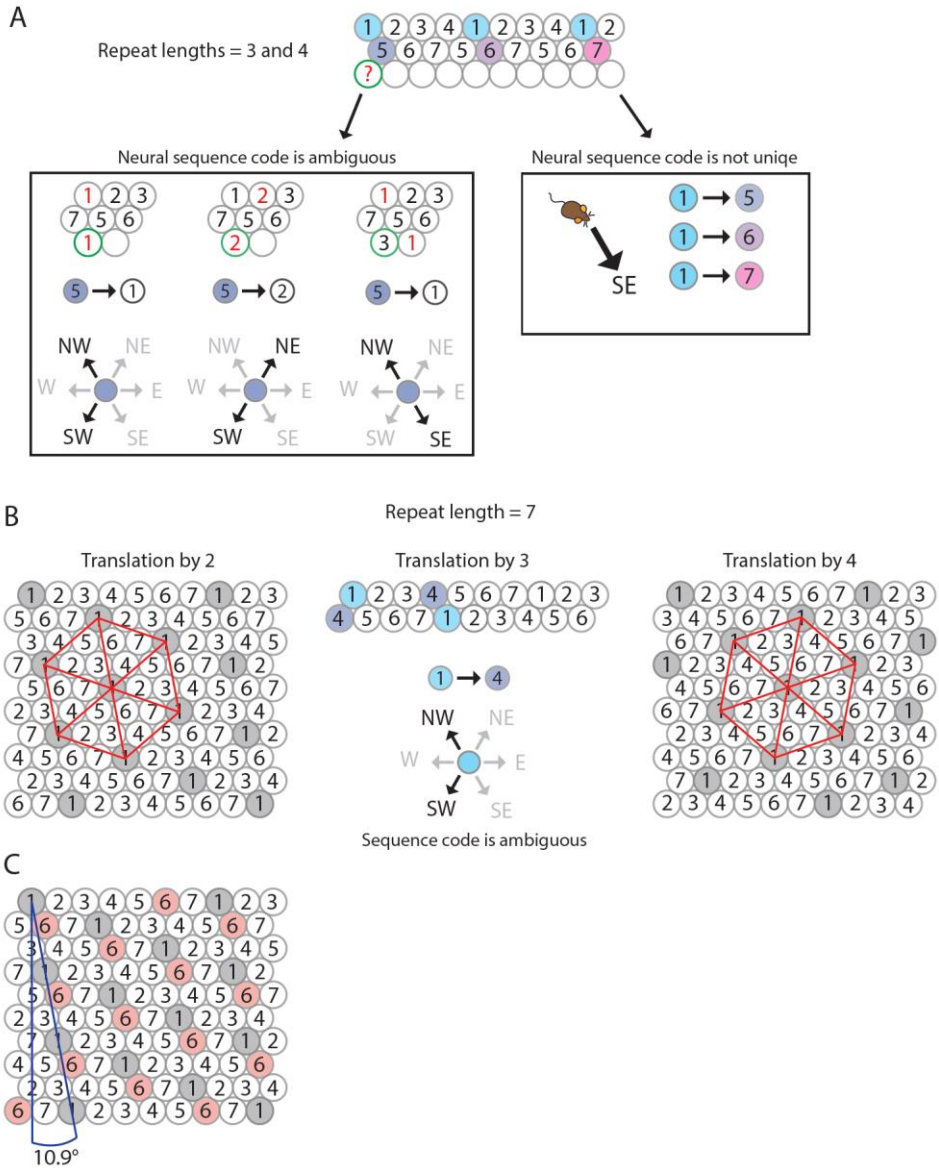

Figure 3. The minimum number of distinct cells providing a sequence code of trajectories in 2D space is 7, and there are exactly 2 possible arrangements of the cells' firing fields up to relabeling. A, Repeat lengths that are smaller than 7 result in a violation of cell sequence coding of trajectories because the resulting code is ambiguous and not unique. A red question mark indicates that no cell can be found for this position that would not violate the sequence code. Red numbers indicate that activity of this cell at the current position would violate sequence coding of trajectories due to ambiquity. Blue background color marks the sequential activity of 2 cells that violate cell sequence coding of trajectories (Definition 8) because the next active cell is not uniquely determined by the currently active cell in the sequence and the velocity vector associated with the current trajectory. **B**, If the repeat length is 7, there are three potential translations of the sequence in row 1 to fill up row 2 (Lemma 13.1). Only two of those three tranlsations result in an arrangement of cells (up to relabeling of cells) that creates a sequence code for trajectories in 2D space. These two arrangements are mirror images of each other (up to relabeling) and imply that the firing fields of each individual grid cell fall on the vertices of equilateral triangles, i.e., they form a hexagonal grid. **C**, Both possible arrangements of firing fields imply that grid patterns of other grid cells have the same spacing and rotation, and only differ in spatial phase (compare grid patterns of cell #1 and cell #6). The smallest angle between one grid axis and the boundary of a rectangular enclosure is 10.9 degrees if one sequence of cells is aligned with one of the borders of the enclosure.

Figure 4

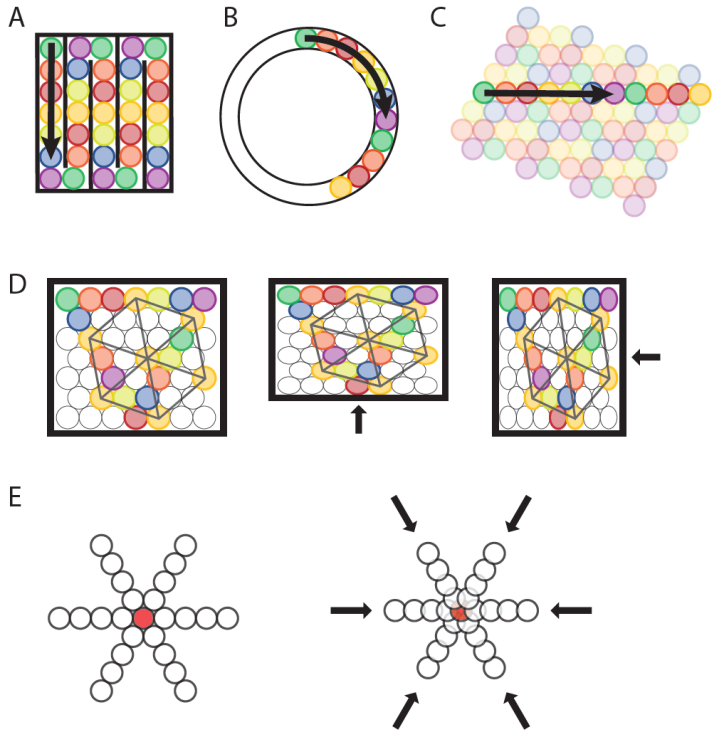

Figure 4. Transformation of a cell sequence code of trajectories from 2D space to 1D space. A,**B**, A sequence of 7 different cells can code for a trajectory in a 1D compartmentalized "hairpin" maze (A) or a 1D circular track (B). Note that the distance between firing fields would increase in the 1D "hairpin" maze and 1D circular track compared to the distance between spatial firing fields in a 2D environment. Also note that cell sequences could undergo a phase reset at behaviorally relevant points, e.g., the turning points in the "hairpin" maze (A). **C**, The sequence of active cells in a 1D environment can be interpreted as a cross-section of the trajectory sequence code in a 2D space. **D**, Anchoring of firing filelds to environmental borders predicts parametric rescaling of an individual cell's grid pattern when a familiar enclosure is deformed. Each color represents one grid cell, each circle represents one firing field. For clarity, the complete set of firing fields of a single cell is shown only for one grid cell shown in orange. In addition, grid cell sequences are shown for all three major axes. Left panel, original maze configuration. Mid and right panel, the environment is compressed along the vertical or horizontal dimension resulting in a parametric deformation of firing fields and the grid pattern of firing fields along the vertical or horizontal dimension. **E**, Progressively faster advancement from the current active cell to the next active cell in the sequence code of trajectories results in progressive decrease in grid spacing and thereby a local distortion of the grid map. Open circles represent firing fields of grid cells along the three major axes. The red filled circle in the center represents a salient location such as a rewarded goal location toward which nearby grid fields gravitate.

Figure 5

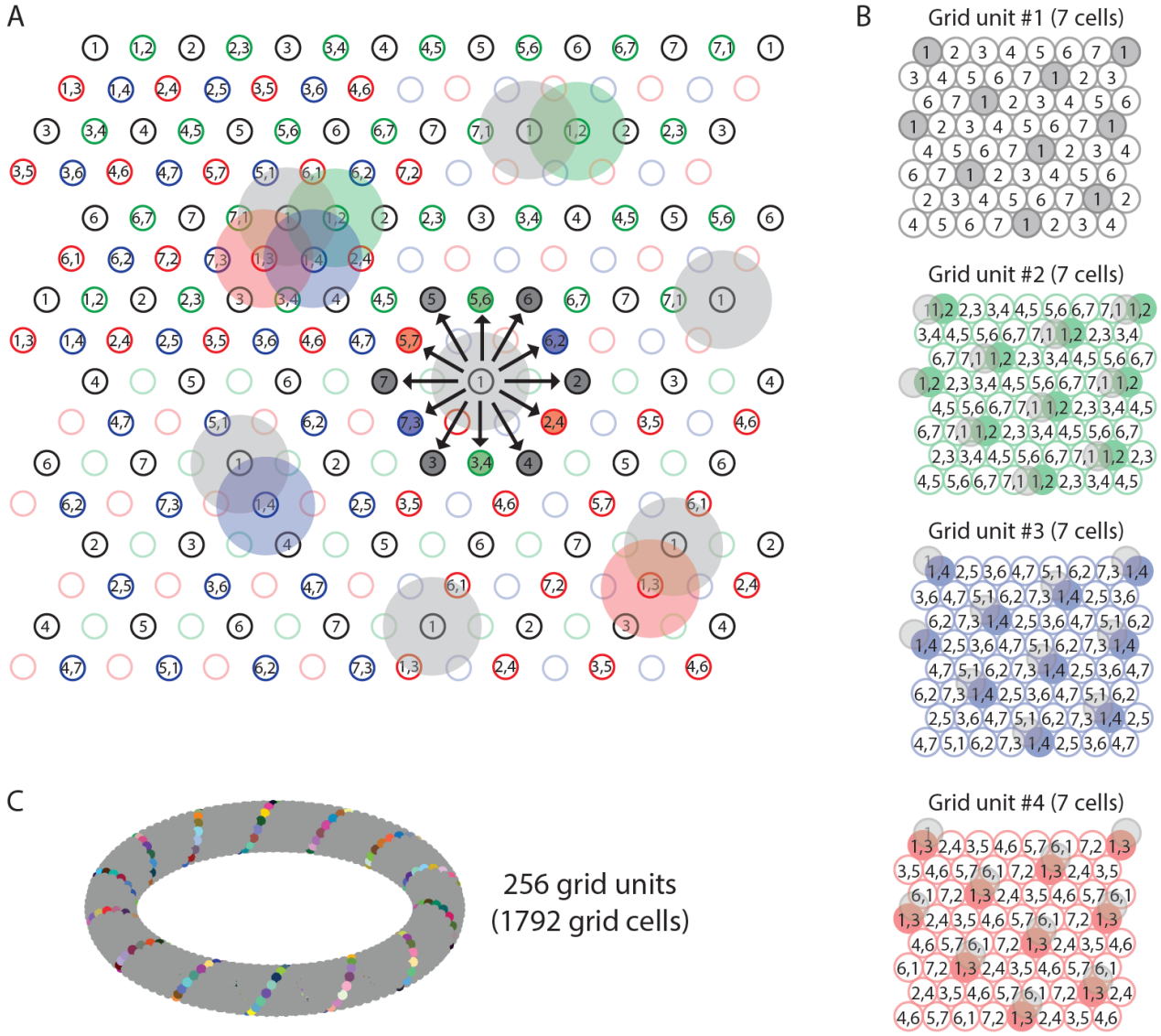

Figure 5. Multiple grid units provide nearly continuous resolution in the coding of trajectories. A, The circles with numbers show the *centers* of the grid fields of a total of 28 grid cells from four fundamental grid units, each consisting of seven grid cells. Cells from each grid unit are shown with the same color (black, green, blue, and red). The grid fields of the grid unit shown in green are phase-shifted along the horizontal axis, the fields of the grid unit shown in blue are phase-shifted along one of the two major diagonal axes, the fields of the grid unit shown in red are phase-shifted along the other diagonal axis. Each number (e.g., "1") or combination of number (e.g., "1,2" represents one grid cell). For better clarity, not all numbers are shown. A combination of numbers indicates that the grid field centers fall in between the fields of two neighboring grid cells. E.g., the field centers of cell "1,2" fall in between the field centers of cells "1" and "2". The full transparent circles represent the full-sized field. For visualization purposes, only six full-sized fields are shown for cell "1", and two fields each for cells "1,2", "1,3", and "1,4". **B**, The non-overlapping grid fields of the seven grid cells for each of the four fundamental grid units shown in A. The grid pattern is highlighted in color for one grid cell in each unit. The phase-shift to the other grid cells is indicated by showing the transparent grid pattern of cell "1". **C**, When more grid units are added, the grid cells can be represented in 3D as a neural manifold, shown here for a total of 1792 grid cells from 256 grid units. The colored cells represent one diagonal axis across rows of non-repeating cells when plotting the cells as shown in A.

TABLES

Table 1

	Axiom	Remark/Example
Axiom 1	Cell sequences code for trajectories in 2D space.	This axiom states that the sequential activity of two cells, e.g., i → j, can unambiguously be interpreted by a downstream reader mechanism as a a code for one and only one trajectory, e.g., moving from place A to place B.
Axiom 2	The reverse cell sequence codes for the reverse trajectory.	If the cell sequence i → j codes for moving from place A to B, then the reverse cell sequence j → i codes for moving from place B to place A.
Axiom 3	Each cell's firing field is surrounded symmetrically by a maximal number of other cell's firing fields so that the angular resolution is constant and maximal across all directions.	This axiom means that a sequence code should represent each direction equally with no "gaps" in the representation (**Figures 3D-E**).
Axiom 4	The number of cells is finite.	Grid cells are densest in layer II of the medial entorhinal cortex [75], and this layer has been estimated to contain 24,000 and 58,000 neurons in mice and rats, respectively [76].

Table 1. Axioms from which grid cell firing emerges as the most parsimonious solution to provide a code for trajectories in 2D space.

Table 2

# neurons	Repeat lengths[a]	Lattice type	Smallest angle to a border of a rectangular environment[b]
7	7, 7, 7	Hexagonal	10.9°
8	4, 8, 8	Centered rectangular	0°
	4, 8, 8	Oblique	10.9°
9	3, 3, 3	Hexagonal	0°
	3, 9, 9	Oblique	10.9°
	3, 9, 9	Oblique	13.9°
	3, 9, 9	Oblique	16.1°
10	5, 10, 10	Oblique	0°
	5, 10, 10	Oblique	10.9°
	5, 10, 10	Oblique	16.1°
11	11, 11, 11	Oblique	6.6°
	11, 11, 11	Oblique	10.9°
	11, 11, 11	Oblique	16.1°
12	6, 6, 6	Hexagonal	0°
	3, 12, 12	Rectangular	0°
	3, 12, 12	Rectangular	10.9°
	3, 4, 12	Oblique	0°
	3, 4, 12	Oblique	13.9°
	4, 6, 12	Oblique	0°
	4, 6, 12	Oblique	6.6°
	4, 6, 12	Oblique	23.4°

Table 2. List of possible grid maps and properties of these grid maps given the total number of neurons participating in a trajectory-coding sequence in a rectangular environment. For each grid map that has a non-zero angle to a border, a reflection or 90°-rotation and reflection up to relabeling of the cells exist, and these additional possibilies are not included in this list.

[a]Repeat lengths across the three major axes of the hexagonal lattice structure of densely packed firing fields.

[b]The smallest angle to a border of a rectangular environment assumes that one sequence of cells is arranged in parallel to one wall.

BOXES

Box 1. Math notations:

A *lemma* is a mathematical statement that will be used to prove another result.

A *proposition* or *theorem* is a mathematical statement that can be proved using logical deduction from previously known results.
A *proof* is a logical argument using known results to generate new mathematical statements. The purpose of a proof is to convince the reader that the result follows from known results.

A *plane* is a flat surface extending infinitely far in two dimensions. Also referred to as $\mathbb{R}^2$, since it can be assigned coordinates of the form (a, b) where a and b are real numbers.

A *Euclidean metric* is the usual notion of distance in the plane. Two points with coordinates (x_1, y_1) and (x_2, y_2) have distance $\sqrt{(x_1 - x_2)^2 + (y_1 - y_2)^2}$.

Adding points means adding their coordinates, *subtracting one point from another* involves subtracting their coordinates.

A *bijective map* is a correspondence between two sets such that every point in one set is matched with exactly one point in the other set.

A *geometric figure* is a geometric object with a shape in the plane.

We work in $\mathbb{R}^2$ (the plane), with the Euclidean metric.